

Tuning photoluminescence of ZnS nanoparticles by silver

A MURUGADOSS¹ and ARUN CHATTOPADHYAY^{1,2,*}

¹Department of Chemistry and ²Centre for Nanotechnology, Indian Institute of Technology Guwahati, Guwahati 781 039, India

Abstract. We report the results of investigation of the interaction of silver with presynthesized ZnS nanoparticles (NPs) that was stabilized by cetyl trimethyl ammonium bromide (CTAB). The photoluminescence properties of ZnS NPs were followed in the presence of Ag⁺ ions, Ag NPs and by the synthesis of Ag@ZnS core-shell nanoparticles. We observed that CTAB stabilized ZnS NPs emitted broadly in the region from 350–450 nm, when excited by 309 nm light. In the presence of Ag⁺ ions the emission peak intensity up to 400 nm was reduced, while two new and stronger peaks at 430 nm and 550 nm appeared. Similar results were obtained when Ag NPs solution was added to ZnS solution. However, when Ag@ZnS NPs were synthesized, the emission in the 350–450 nm region was much weaker in comparison to that at 540 nm, which itself appeared at a wavelength shorter than that of Ag⁺ ion added ZnS NPs. The observations have been explained by the presence of interstitial sulfur and Zn²⁺, especially near the surface of the nanocrystals and their interaction with various forms of silver. In addition, our observations suggest that Ag⁺ ions diffuse into the lattice of the preformed ZnS NPs just like the formation of Ag⁺ doped ZnS NPs and thus changes the emission characteristics. We also have pursued similar experiments with addition of Mn²⁺ ions to ZnS and observed similar results of emission characteristics of Mn²⁺ doped ZnS NPs. We expect that results would stimulate further research interests in the development of fluoremetric metal ion sensors based on interaction with quantum dots.

Keywords. Nanoparticles; photoluminescence; silver; zinc sulfide; doping.

1. Introduction

The search for the development of efficient photocatalyst working in the visible region of light has led to the development of hybrid materials, where one component of the structure is generally made up of semiconductor nanoparticles (NPs) (Henglein 1989; Kenemoto *et al* 1992; Hamanoi and Kudo 2002; Hu *et al* 2005; Ipe *et al* 2005). ZnS, ZnSe, CdS and CdSe nanocrystals (NCs) are some of the examples that figure prominently in the list of such semiconductor materials (Wang and Herron 1991; Pradhan and Efrima 2003; Song *et al* 2005; Yutaka *et al* 2005; Zhang *et al* 2005). The primary concern in this regard has been in achieving a hybrid system where the semiconductor NPs would be doped with metal ions in order to tune the optical and catalytic properties of NPs (Backer and Bard 1983; Yanata *et al* 1993; Bhargava *et al* 1994; Sooklal *et al* 1996; Borse *et al* 1999; Lingdong *et al* 1999; Wei *et al* 2000; Karar *et al* 2004; Yang *et al* 2005; Borse *et al* 2006). For example, CdS NPs have been doped with Mn²⁺ ions in order to achieve fluorescence in the visible region with application in sensing especially biological sensing (Counio *et al* 1996; Bruchez *et al* 1998; Mingyoung *et al* 2000; Tridade *et al* 2001; Bool *et al* 2003). On the other hand, ZnS NPs when doped with Ag⁺ ions

exhibit intense fluorescence in the visible region at 550 nm that increases with the dopant concentration (Hao *et al* 1998; Jungsik *et al* 2004). However, there is no report of systematic tuning of the fluorescence wavelength of the semiconductor by addition of metal ions after the synthesis of the semiconductor NPs. This is important as the tuning can easily be externally controlled by suitable choice of added metal ion concentration. Also, if the fluorescence can be tuned by specific metal ions, it could form the basis of detection of metal ions using quantum dots (Qdots).

Herein we report the results on the change in the photoluminescence of ZnS upon incorporation of silver. The silver incorporation was carried out in the form of addition of either Ag⁺ ions or Ag NPs directly to the aqueous solution containing ZnS NPs. In addition, syntheses of Ag@ZnS core-shell NPs were carried out. We observed that upon addition of Ag⁺ ions the fluorescence of ZnS at 350–400 nm disappeared gradually while strong fluorescence appeared at two wavelengths, one at 430 nm and the other at 550 nm. On the other hand, when Ag@ZnS NPs were prepared, the fluorescence at 550 nm was significantly higher than that in the region of 350–450 nm and no special peak at 430 nm appeared. Additionally, the addition of Ag NPs solution had a mixed effect of Ag⁺ ions and Ag NPs. Similar experiments performed with the addition of Mn²⁺ indicate that the metal ions diffuse into the crystal lattice of ZnS giving rise to extraordinary properties of fluorescence.

*Author for correspondence (arun@iitg.ernet.in)

2. Experimental

2.1 Materials

Zinc acetate (99%, Merck), sodium sulfide (58%, Merck), silver nitrate (99.5%, Merck), sodium borohydride (95%, Merck), manganese acetate ($\text{Mn}(\text{OAc})_2 \cdot 4\text{H}_2\text{O}$; 99%, CDH Laboratory) and CTAB (cetyl trimethyl ammonium bromide, 99% Aldrich) were used as received without further purification. Milli-Q grade water was used in all experiments.

2.1a Synthesis: (I) *ZnS@Ag NPs*: 218.7 mg of CTAB was dissolved in 50 mL of water and the solution was then stirred for 30 min at room temperature. The following procedures were then followed in order to synthesize *ZnS@Ag* core-shell NPs with different proportions of ZnS and Ag.

Experiment 1: 0.1 mM of AgNO_3 was added to the above solution while it was being stirred. This was followed by addition of sodium borohydride (0.032 mM) to the solution. The resulting solution appeared brown in colour, which is indicative of the formation of Ag NPs. 33.5 mg of zinc acetate and 40.36 mg of sodium sulfide were then added to the mixture. The stirring was continued for 8 h at room temperature. Finally, the solution was strong yellow in colour.

Experiment 2: 0.08 mM of AgNO_3 was added to the above solution while it was being stirred. This was followed by addition of sodium borohydride (0.024 mM) to the solution. The resulting solution appeared brown in colour, which is indicative of the formation of Ag NPs. 33.5 mg of zinc acetate and 40.36 mg of sodium sulfide were then added to the mixture. The stirring was continued for 8 h at room temperature. Finally, the solution was yellow in colour, however, weaker than that obtained in experiment 1.

Experiment 3: 0.06 mM of AgNO_3 was added to the above solution while it was being stirred. This was followed by addition of sodium borohydride (0.02 mM) to the solution. The resulting solution appeared brown in colour, which is indicative of the formation of Ag NPs. 33.5 mg of zinc acetate and 40.36 mg of sodium sulfide were then added to the mixture. The stirring was continued for 8 h at room temperature. Finally, the solution was yellow in colour, however, weaker than that obtained both in experiments 1 and 2.

(II) *ZnS NPs preparation followed by addition of AgNO_3 at several concentrations*: 218.7 mg of CTAB was dissolved in 50 mL water and the solution was stirred for 30 min at room temperature. This was followed by addition of 33.5 mg of zinc acetate and 40.36 mg of sodium

sulfide and stirring was continued. Four such solutions were prepared in separate flasks. After 1 h, 5 mL (experiment a), 10 mL (experiment b), 15 mL (experiment c) and 20 mL (experiment d) portions of solution containing 0.06 mM AgNO_3 and 0.06 mM CTAB in water were added separately. The stirring was continued for 8 h at room temperature (varied between 25 and 35°C).

(III) *ZnS NPs preparation followed by addition of Ag NPs at several concentrations*: Ag NPs synthesis: 0.06 mM of AgNO_3 was added to 50 ml of 0.06 mM of CTAB solution in water which was followed by addition of 0.2 mM of sodium borohydride. The solution was stirred at room temperature and it became strong yellow in colour formed within a minute indicating the formation of Ag NPs.

ZnS NPs synthesis: 218.7 mg of CTAB was dissolved in 50 mL water and the solution was stirred for 30 min at room temperature. This was followed by addition of 33.5 mg of zinc acetate and 40.36 mg of sodium sulfide and stirring was continued. Four such solutions were prepared in separate flasks.

Mixing the two: After 1 h of stirring of the ZnS NPs solution, 5 mL (experiment 1), 10 mL (experiment 2), 15 mL (experiment 3) and 20 mL (experiment 4) portions of solution containing Ag NPs as above were separately added to four separate solutions containing ZnS NPs. The stirring was continued for 8 h at room temperature (varied between 25 and 35°C).

(IV) *ZnS preparation followed by addition of $\text{Mn}(\text{OAc})_2$* : The preparation of ZnS was pursued using the protocol mentioned in (II). After 1 h of preparation, 5 mL of solution containing 0.15 mM $\text{Mn}(\text{OAc})_2$ was added. The stirring was continued for 8 h at room temperature (varied between 25°C and 35°C).

3. Results and discussion

In figure 1, we show the results of UV-vis studies of ZnS NPs stabilized by CTAB and also the effect of addition of Ag^+ ions, Ag NPs and the formation of *Ag@ZnS* core-shell NPs. The UV-vis spectrum of ZnS consisted of a peak at 309 nm, which corresponds to a bandgap of 4.01 eV. The UV-vis spectra of all other samples treated with silver appeared to be similar. This indicates that the basic characteristics of the ZnS NPs bandgap were not affected by treatment with silver. In other words, the addition of Ag^+ or Ag NPs did not change the absorption characteristic of ZnS. Also the ZnS shell in the *Ag@ZnS* core-shell NPs exhibited absorption characteristics similar to that of ZnS only or Ag treated ZnS NPs. However, it is interesting to note that the peak intensity at 309 nm

diminished with the addition of silver in all cases thus indicating the effect on the oscillator strength of the Qdots. Also, since the concentration of Ag NPs added in here was small there is no significant evidence of addi-

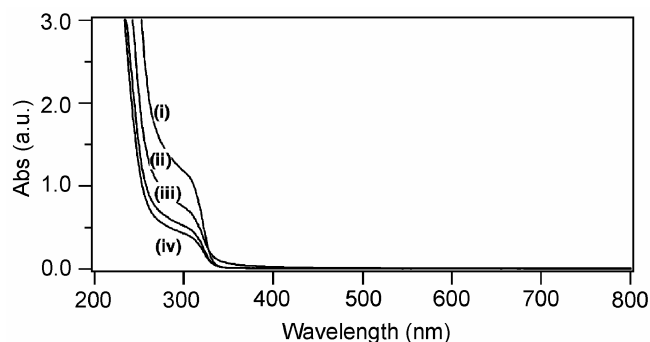


Figure 1. UV-vis spectra of (i) ZnS only, (ii) Ag@ZnS NPs as in experiment 1 of (I), (iii) ZnS and 20 ml of Ag NPs, (III) and (iv) ZnS and 20 ml of AgNO₃ as in (II).

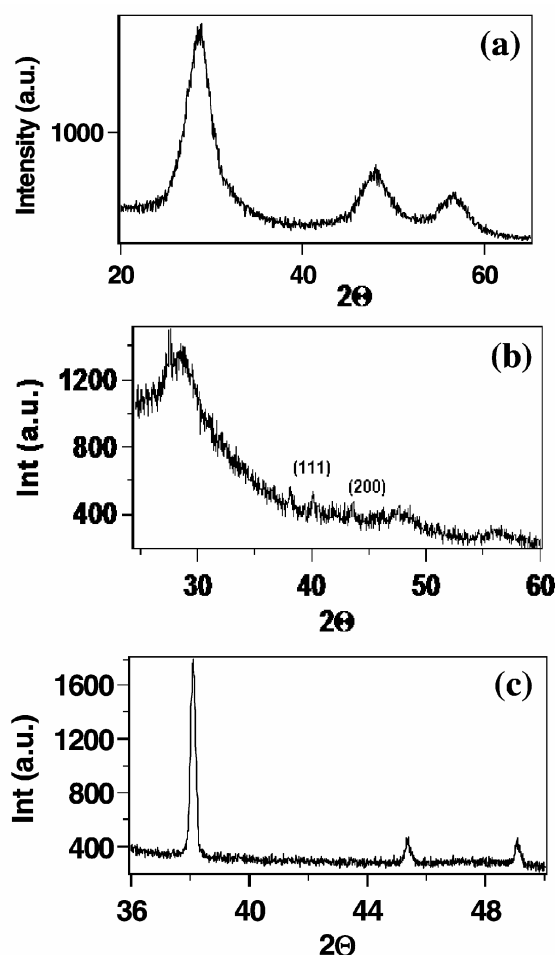


Figure 2. (a) X-ray diffraction pattern of CTAB stabilized ZnS NPs, (b) core shell Ag@ZnS particles and (c) is the expanded view of (b) in the region 36° to 50°. X-ray diffractions were recorded in thin film mode.

tional absorption due to added NPs. Further, in the case of Ag@ZnS core-shell NPs the characteristic absorption due to ZnS is evident as it forms the shell and due to the presence of the shell the absorption owing to Ag was not observed.

The X-ray diffraction of ZnS (figure 2) prepared using the present method showed three prominent and broad peaks at 28.8° (due to {111} planes), 48° (due to {220} planes) and at 56.8° (due to {311} planes). The average particle sizes calculated from the peaks are 3.7 nm, 4.2 nm and 4.7 nm, respectively (Yang *et al* 1996; Liz-Marsan 2006). Thus small NPs of ZnS could be produced using the present method of synthesis in the presence of CTAB as the stabilizer. Similarly, the XRD patterns of Ag@ZnS showed the characteristic peaks of Ag and ZnS indicating that both were present in the core-shell NPs (figure 2b) (Yang and Ly 2005). Also, no clear XRD peak due to additional Ag⁺ or Ag NPs was observed, when the solution containing either of the species was added to the solution of ZnS NPs, except that the peaks due to ZnS became weaker with more addition of either of them. This could be due to successive dilution of the solution containing ZnS NPs upon addition of solution of Ag⁺ or Ag NPs. We would like to mention here that in many cases we observed that the peaks due to CTAB

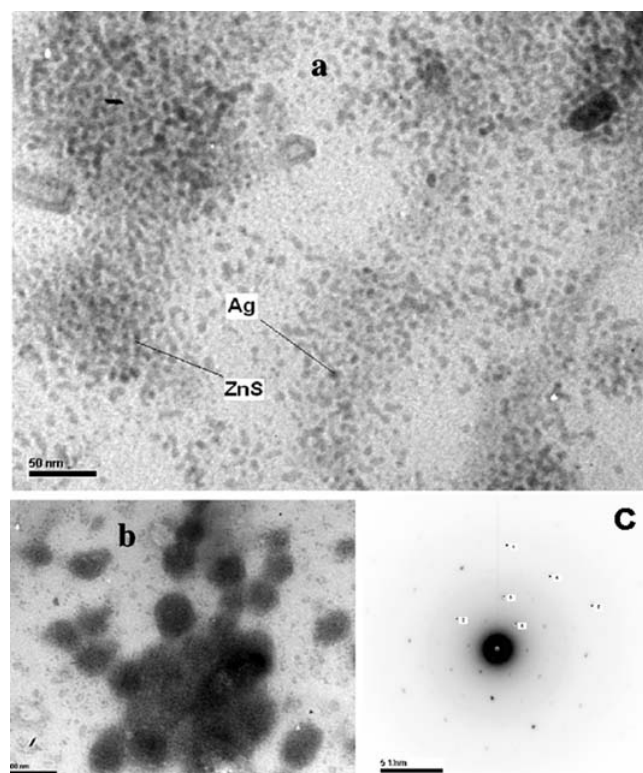


Figure 3. (a) Transmission electron micrograph of CTAB stabilized Ag@ZnS NPs. Darker spots are due to Ag and lighter rods are due to ZnS, (b) an expanded view of the NPs showing the presence of core-shell particles and (c) selected area electron diffraction (SAED) of core Ag and shell ZnS nanoparticles.

overwhelmed the peaks of the NPs when the film was formed by evaporation of the solution, which also could be a reason for the above observation.

As a typical example, we show the transmission electron micrograph (TEM) of Ag@ZnS NPs in figure 3a. As evident from the figure, the Ag@ZnS showed the presence of spherical Ag core surrounded by rod-shaped ZnS nanoparticles (figure 3). The particles formed were nearly uniform with sizes typically 20 nm in diameters. A better view of the core-shell particles can be obtained in figure 3b. Further the selected area electron diffraction pattern for the core shell of Ag@ZnS is shown in figure 3c.

The fluorescence spectroscopic measurements of ZnS only NPs (figure 4A) showed a broad peak in between the region of 325 nm and 430 nm, when excited by light at 309 nm. However, two prominent and sharp peaks at 360 nm and 430 nm could be clearly seen superimposed in the emission spectrum. On the other hand, when Ag@ZnS NPs were excited by the same light a strong peak at 540 nm appeared while the peaks in the region of 350–450 nm diminished. The results are shown in figure 4B. In addition, another peak at 430 nm could also be observed.

We were further interested in investigating the effect of Ag⁺ and/or Ag NPs on the emission spectrum of ZnS. For this, we added several proportions of AgNO₃ solution or

Ag NPs (previously prepared) containing solutions to the ZnS solution. This was followed by subsequent recording of emission spectra with excitation at 309 nm. Figure 5A shows the spectra of ZnS upon the addition of Ag⁺ ions (solution) at several concentrations. The intensity due to ZnS only in the region 350–400 nm reduces with addition of Ag⁺ and subsequently intensity of the peak at 430 nm was greatly enhanced, while another peak appeared at 550 nm. Further addition of Ag⁺ leads to increase in the intensity of 550 nm peak, while no change in either in the region at 350–400 nm as well as the intensity of the 430 nm peak. We report the effect of addition of Ag NPs on the fluorescence spectra of ZnS NPs. The results are shown in figure 5B. The results here are quite interesting. First of all just like the addition of Ag⁺, the intensity of the peaks in the region 350–400 nm did not increase, while peak at 430 nm was enhanced. However, the peak at higher wavelength is much broader encompassing the region of both 540 nm and 550 nm peaks observed in the case of formation of Ag@ZnS and the effect of addition of Ag⁺ ions to ZnS as in figures 4A and B, respectively. Also, one could observe the relative increase in intensity at 550 nm in comparison to 540 nm, while the increase at 450 nm was less prominent at the first two concentrations of Ag NPs. This effect could be a combination of Ag NPs and Ag⁺ ions that could be present in the solution of Ag

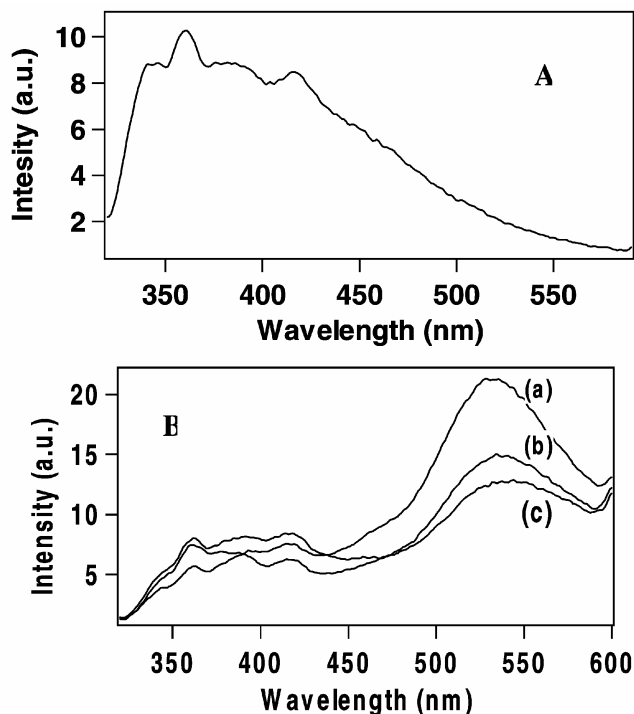


Figure 4. **A.** Fluorescence spectrum of ZnS NPs and **B.** fluorescence spectra of Ag@ZnS NPs with the ratio of AgNO₃ and Zn (OAc)₂, (a), (b) and (c), being the results of experiments 1, 2 and 3, respectively in (I). The excitation wavelength used was 309 nm in both the cases.

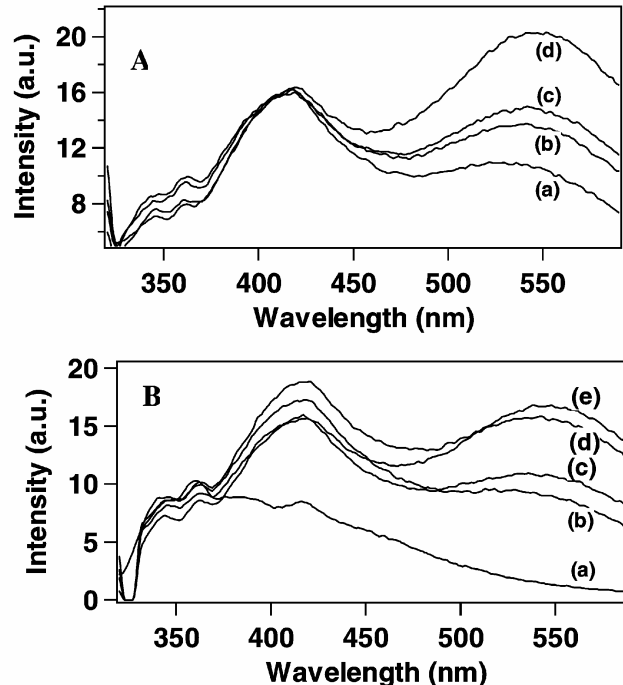


Figure 5. **A.** Fluorescence spectra of ZnS NPs upon addition of (a) 5 mL of 0.06 mM AgNO₃, (b) 10 mL of 0.06 mM AgNO₃, (c) 15 mL of 0.06 mM AgNO₃, (d) 20 mL of 0.06 mM AgNO₃ and **B.** fluorescence spectra of (a) ZnS NPs and then its changes upon addition of (b) 5 mL of Ag NPs, (c) 10 mL of Ag NPs, (d) 15 mL of Ag NPs, (e) 20 mL of Ag NPs as in (III).

NPs as unreacted ions. Thus the effects of both Ag NPs and Ag^+ ions could be seen in the addition of Ag NPs to ZnS NPs solution.

In order to understand the effect of addition of silver onto the ZnS NPs the fluorescence spectrum of ZnS in the presence of additional Mn^{2+} , prepared similar to the way Ag^+ ions were added, was deemed helpful. The result of addition of 5 mL of 0.15 mM $\text{Mn}(\text{OAc})_2$ is shown in figure 6. There are two important effects that need to be observed. First of a strong peak appeared at 430 nm while an additional weak peak appeared at 580 nm. The peak at 580 nm is characteristic of Mn^{2+} doped ZnS NPs as reported in previous studies. This indicates that in the process of addition of metal ions to ZnS and stirring for long hours, metal ions not only interact with the outer surfaces of the Qdots, they also diffuse into the crystal of individual Qdots thereby changing the optical properties of pure ZnS into a doped one. Similar cases may be happening when Ag^+ are added to ZnS NPs solution. The details of interpretation of the results are given below.

It is well established that in semiconductor NPs the photoemissions occur by the recombination of electrons and holes, which are the photo excited carriers, via various paths. They could be direct band–band recombination, recombination via shallow trap states or via deep trapped states of different kind. In a semiconductor like ZnS, with a bandgap energy of 4.01 eV, there are several states from or to which emission can occur. These are schematically shown in figure 7A. First of all there can be an emission from the conduction band edge (Stokes shift) which will be close to the absorption wavelength (Dunstan *et al* 1990; Chae *et al* 2004). There can also be emissions from the conduction band (CB) to the interstitial sulfur or vacant states of Zn^{2+} . On the other hand, the presence of interstitial Zn^{2+} and vacant sulfur would also give rise to emissions at different wavelengths. In the present case when ZnS, stabilized by a surfactant (CTAB), was excited at 309 nm, a broad emission in the region 325–550 nm, with several peaks in between, was observed.

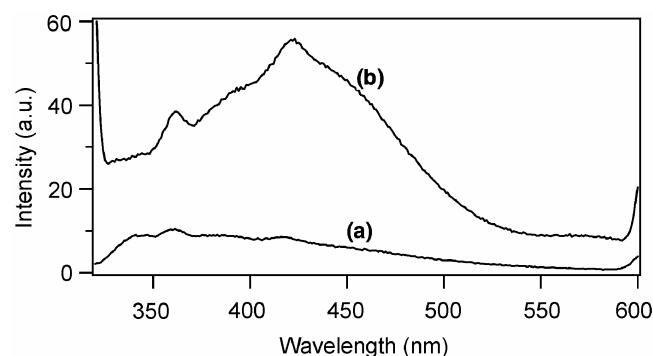


Figure 6. Fluorescence spectrum of ZnS upon treatment with $\text{Mn}(\text{OAc})_2$ as in experiment (IV). (a) ZnS NPs only and (b) was recorded after addition of $\text{Mn}(\text{OAc})_2$ into ZnS NPs solution.

These emissions occur due to the presence of interstitial sulfur, Zn^{2+} and vacancies due to Zn^{2+} and S^{2-} . This emission band primarily vanished gradually with the addition of Ag^+ , while the peak at 430 nm became intense and a new peak at 550 nm appeared. The peak at 430 nm did not change with more additions of Ag^+ ions while the peak at 550 nm continued to increase. Thus the peak at 430 nm is probably due to the presence of sulfide ion vacancies which was created by the addition of excess Ag^+ ions. Additional presence of sufficient Ag^+ ions did not change further the sulfur vacancy sites (probably due to stability of NPs) and thus then there was no increase in the peak at 430 nm with further addition of Ag^+ . On the other hand, the peak at 550 nm is possibly due to the presence of Ag centres, the concentration of which increased with the increase of Ag^+ ions, and thus the number of acceptors increased. Hence, the peak at 550 nm continued to increase with the addition of Ag^+ ions.

When Ag NPs solution prepared separately, was added to the solution containing ZnS NPs, the peak at 360 nm had vanished and two new peaks at 430 nm and a broad peak encompassing 540 nm and 550 nm appeared. It is important to note that at the lower concentration of added Ag NPs the peak was primarily at 540 nm and with the addition of further Ag NPs solution the peak at 550 nm became more prominent along with the peak at 540 nm. Also, with the increase in the concentration of Ag NPs the peak at 430 nm increased. The explanation is as follows. In general, in the solution of Ag NPs there would be excess Ag^+ ions, which would interact with ZnS NPs in much the same way as the added Ag^+ ions. However, since the concentration of Ag^+ ions in Ag NPs solution is comparatively less with respect to addition of direct Ag^+ ions, the peak at 430 nm and 550 nm would gradually increase, with preference towards introduction of sulfur vacancy sites (and thus increase in 430 nm emission first). The peak at 540 nm is due to the presence of Ag NPs. This means that the interaction of Ag NPs at the surface of ZnS leads to an emission at 540 nm with probably

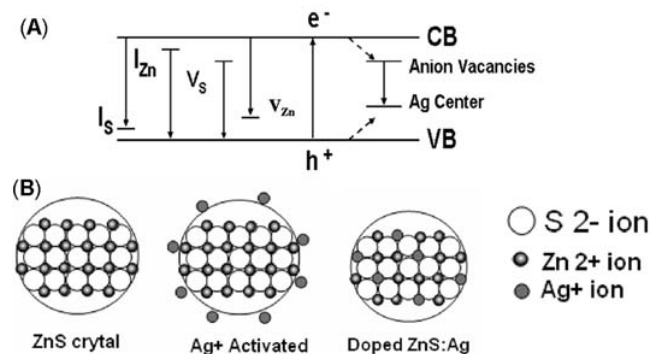


Figure 7. (A) A schematic energy diagram of ZnS NPs energy states with various defects and (B) schematics of defects that typically may occur in the present set of experiments.

the Ag NPs acting as acceptors. This can easily be seen in the case of the preparation of Ag@ZnS NPs (figure 4B) where the peak at 540 nm was prominent and all other peaks were either absent (especially at 550 nm) or weak in intensity. Thus Ag NPs clearly act as fluorescence enhancers of 540 nm emission, which is due to the Ag present at the periphery of the ZnS NPs either when Ag NPs are added (on the outer surface of ZnS) or when Ag@ZnS NPs are prepared (Ag NPs present at the inner surface of ZnS shell). Again, with the addition of further Ag NPs solution the number of Ag⁺ ions increases and when the concentration of Ag⁺ is sufficient to introduce excess ions into the crystal of ZnS then there are enough acceptors to induce the emission at 550 nm. Thus the peak at 540 nm and 550 nm merge and a broader peak appears. Hence, the present method has the option of tuning emission intensities as well as wavelengths by appropriately choosing the addition of Ag⁺ ions or Ag NPs and associated Ag⁺ ions present in the solution. It may be mentioned here that there is a chance of formation of Ag₂S by reaction of ZnS with Ag⁺. We have observed that if Ag₂S NPs are synthesized separately there is no characteristic fluorescence from the particles that would overlap with the observed fluorescence in the above cases. Hence, fluorescence due to the presence of Ag₂S may not be important here.

The results of the study with Mn²⁺ additions to the prepared ZnS agree well with those of above explanations with respect to addition of silver to ZnS. For example, it has been observed that Mn²⁺ doped ZnS NPs emits at 575 nm, which is same as the one we have observed after addition of Mn²⁺ ions to ZnS NPs. The emission is due to the transition ⁴T₁ – ⁶A₁. This means when Mn²⁺ ions are added to ZnS solution, the ions diffuse into the interstitial spaces of already formed ZnS nanocrystals and give rise to emissions characteristics of doped ions or the presence of metal centres and also result in the creation of sulfur vacancies (Backer and Bard 1983; Bhargava *et al* 1994; Sooklal *et al* 1996; Karar *et al* 2004). The sulfur vacancies give rise to emission at 420 nm similar to that due to addition of Ag⁺ ions to ZnS Qdots. This is interesting as we have a method not only of introduction of metal ions into the crystals of Qdots but also a simple way of tuning their fluorescence and thus basically have a method of possible quantitative detection of ions in solution by fluorescence.

4. Conclusions

In brief, we have been able to show that the fluorescence of ZnS NPs (stabilized by CTAB) can be tuned by interaction with silver in three different ways, viz. with Ag⁺, Ag NPs and Ag@ZnS core-shell NPs. This was mainly achieved by external addition of silver species after the preparation of ZnS NPs. The results of emissions match with the hypothesis that metal ions diffuse into the crystal

lattice of ZnS to introduce metal centres and also effect the removal of interstitial sulfur. This conclusion is consistent with the observation of fluorescence upon addition of Mn²⁺ ions into ZnS NPs solution, which is characteristic of the presence of doped Mn²⁺ ions in the ZnS NPs. Although tuning of fluorescence has been observed with respect to introduction of metal ion impurities at the preparation stage, the observations made in the present set of studies have not been reported earlier. Finally, one can envisage that the present method could be the basis of using quantum dots like ZnS as inorganic ions sensors, especially heavy metal ions, in aqueous solution, which we are currently pursuing.

Acknowledgements

We thank the Department of Science and Technology (DST), Government of India, for financial support (No. SR/S5/NM-01/2005, and DST/TSG/ME/2003/83). One of the authors (AC) is a recipient of Swarnajayanti Fellowship Award (2/2/2005-S.F.) of DST.

References

- Backer W G and Bard A J 1983 *J. Phys. Chem.* **87** 4888
- Bhargava R N, Gallagher D, Hong X and Nurmikko A 1994a *Phys. Rev. Lett.* **72** 416
- Bhargava N R, Gallagher D and Welker T 1994b *J. Lumin.* **60&61** 275
- Boal A A, Beck R V, Ferwerda J and Meijerink A 2003 *J. Phys. Chem. Solids* **64** 247
- Borse P H, Deshmukh N, Shinde R F, Date S K and Kulkarni S K 1999 *J. Mater. Sci.* **34** 608
- Borse P H, Vogel G and Kulkarni S K 2006 *J. Colloid & Interf. Sci.* **293** 437
- Bruchez M, Moronne M, Gon P, Weiss S and Alivasatos A P 1998 *Science* **281** 2013
- Chae W -S, Yoon J -H, Yu H, Jang D -J and Kim Y -R 2004 *J. Phys. Chem.* **B108** 1150
- Counio S G, Gacoin T E and Boilot J P 1996 *J. Phys. Chem.* **100** 2021
- Dunstan E D, Hagfeldt A, Almgren M, Siegbahn G O H and Mukhtar E 1990 *J. Phys. Chem.* **94** 6797
- Hamanoi O and Kudo A 2002 *Chem. Lett.* 838
- Hao E, Sun Y, Yang B, Zhang X, Liu J and Shen J 1998 *J. Colloid and Interf. Sci.* **204** 369
- Henglein A 1989 *Chem. Rev.* 1861
- Hu J, Ren L, Guo Y, Liang H -P, Cao A -M, Wan L -J and Bai C -L 2005 *Angew. Chem. Int. Ed.* **44** 1269
- Ipe I B and Niemeyer M C 2005 *Angew. Chem. Int. Ed.* **44** 1
- Jungsik A, Billie A, Brent W and Paul H H 2004 *J. Appl. Phys.* **95** 7873
- Karar N, Singh F and Mehta B R 2004 *J. Appl. Phys.* **95** 65
- Kenemoto M, Shiragami T, Pac C and Yanagida S 1992 *J. Phys. Chem.* **96** 3521

- Lingdong S, Changhui L, Chunsheng L and Changhui Y 1999 *J. Mater. Chem.* **9** 1655
- Liz-Marsan L M 2006 *Langmuir* **22** 32
- Mingyoung H, Xiaohu G, Jack Z and Shuming N 2000 *Nature* **405** 923
- Pradhan N and Efrima S 2003 *J. Am. Chem. Soc.* **125** 2050
- Song J -H, Atay T, Shi S, Urabe H and Nurmikko A V 2005 *Nano Lett.* **5** 1557
- Sooklal K, Brain S, Angel M and Murphy C J 1996 *J. Phys. Chem.* **100** 4551
- Tridade T, O'Brien P and Pickett N L 2001 *Chem. Mater.* **13** 3843
- Wang Y and Herron N 1991 *J. Phys. Chem.* **92** 525
- Wei C, Jan-Olle M, Valery Z, Yinging H, Shuman L, Reine W, Jan-Olov B and Lars S 2000 *Phys. Rev.* **B61** 11021
- Yanata K, Suzki K and Oka Y 1993 *J. Appl. Phys.* **73** 4595
- Yang H, Huang C, Su X and Tang A 2005 *J. Alloys and Compounds* **402** 274
- Yang J P, Quadri S B and Ratna B R 1996 *J. Phys. Chem.* **B100** 17255
- Yang X and Ly Y 2005 *Mater. Lett.* **59** 2484
- Yutaka O, Takeo S, Seiji T, Atsushi I and Yoshihiko K 2005 *Appl. Phys. Lett.* **87** 043105/1
- Zhang Z *et al* 2005 *J. Phys. Chem.* **B109** 18352